Characterization of Mg-rich maghemite from tuffite

J. D. FABRIS,* J.M.D. COEY, QINIAN QI, W. N. MUSSEL**

Department of Pure and Applied Physics, Trinity College, Dublin 2, Ireland

ABSTRACT

Maghemite in a tuffite deposit from Patos de Minas, Brazil, has been isolated by high-gradient magnetic separation and analyzed by X-ray diffraction, electron microprobe analysis, Mössbauer spectroscopy, and magnetization measurements. The maghemite constitutes 5 wt% of the tuffite, where it is present as separate grains in the 1–400-μm-size range, some with associated anatase inclusions or intergrowths. The lattice parameter is $a_0 = 0.8380(2)$ nm. No Fe^{2+} is detected, but the composition of the grains shows Fe $\gg$ Mg $\geq$ Ti. The averaged composition and proposed cation distribution is $[Fe_{0.88}Si_{0.01}Mg_{0.11}]$-$\{Fe_{0.96}Mg_{0.30}Ti_{0.32}Al_{0.07}Cr_{0.03}Mn_{0.02}\square_{0.30}\}O_4$, where [ ] and { } denote A and B sites, respectively, of the spinel lattice, and $\square$ denotes cation vacancies. Magnetization, σ_S, is 18–31 J/(T·kg) at room temperature, and the Curie temperature, T_C, is 320–360 °C. The Mg-rich maghemite is inherited by magnetic soils forming on the tuffite.

INTRODUCTION

Maghemite is the cation-deficient ferric spinel with ideal formula $[Fe]\{Fe_{1.67}\square_{0.33}\}O_4$, where the tetrahedral A sites are filled, and vacancies appear mainly on the octahedral B sites. The vacancy structure may preserve a primitive cubic unit cell (Smith, 1979; Goss, 1988) or lead to a superlattice with tetragonal symmetry and $c = 3a$ (Boudeulle et al., 1983; Greaves, 1983). Maghemite is usually formed by low-temperature oxidization of Fe-rich spinel containing Fe^{2+} ions; conversion of one Fe^{2+} ion into Fe^{3+} introduces 0.33 cation vacancies per formula. Oxidation can proceed by addition of O or by expulsion of Fe at the surface.

Ti is the most common substituent for Fe in naturally occurring maghemite. Titanomaghemite has been broadly defined by Lindsley (1976) as any iron titanium spinel lying off the Fe_3O_4-Fe_2TiO_4 join. A principal origin of these minerals is oxidation of a titanomagnetite precursor in, for example, altered submarine pillow basalts found near the midocean ridges (Prévot et al., 1981) or in basalt bedrock from which oxisols are presently forming (Allan et al., 1989). Because the titanomaghemite is substantially more stable against weathering than any other constituent of the basalt, except ilmenite (de Jesus Filho et al., 1994 personal communication), the grains persist throughout the soil profile to give unusual magnetic properties to the soil (Resende et al., 1986). Maghemite containing Al, but no Ti has been found as neoformation products in soils derived from iron dolomite (Moukarika et al., 1991). Maghemite with Ti (Readman and O'Reilly, 1972), Al (Schwertmann and Fechter, 1984), or Zn (Gillot and Benloucif, 1992) substitution has also been synthesized in the laboratory.

Complete characterization of an oxide spinel involves not only determination of the structure and composition but also the cation distribution over A and B sites. Magnetic properties are particularly sensitive to the cation distribution. The magnetization expected from the ideal formula of maghemite for a collinear ferrimagnetic structure, assuming the spin-only value for the ferric moment, is 3.3 Bohr magnetons (μ_B) per formula unit, or $\sigma = 87$ J/(T·kg). If the ferrimagnetic order is maintained, the magnetization will increase at a rate of 5 μ_B per nonmagnetic ion substitution on A sites and decrease at the same rate for nonmagnetic substitution on B sites. In fact, the magnetization of natural maghemite is generally less than the above value, and substitutions of Ti, Al, and Zn all serve to decrease the magnetization. In substituted maghemite, spin canting on B sites because of nonmagnetic substitution on A sites reduces the magnetization further (Allan et al., 1989). Here we describe a natural, predominantly Mg-substituted maghemite found in tuffite from which magnetic soils are forming at present. We report the chemical composition and cation distribution of the new mineral insofar as it can be derived from Mössbauer spectra and magnetization measurements. Its origin and thermal stability are discussed.

OCCURRENCE AND CHARACTERIZATION

The maghemite is present in a tuffite deposit approximately 100 m thick that dates from the Cretaceous period and covers an area of about 5000 km². The greenish-gray tuffite was exposed in a cutting for highway BR365, 23.5 km north of Patos de Minas, Minas Gerais, in the Central Plateau of Brazil. It is covered with an overburden of

TABLE 1. Chemical composition of the tuffite and the magnetically separated extract

	Tuffite*	Magnetic extract**
	wt%	
SiO_2	40.07	0.3(0.2)
Fe_2O_3	22.87	74.6(4.5)
Al_2O_3	5.89	1.8(0.6)
TiO_2	9.43	13.0(2.2)
MgO	5.18	8.4(1.7)
CaO	2.07	
K_2O	3.45	
Na_2O	1.58	
P_2O_5	2.88	
MnO_2	0.55	0.9(0.3)
LOI	7.5	
	ppm	
Cr	789.90	
Ni	1228.41	
Cu	349.48	
Zn	335.23	
Co	303.58	

 * After Fontes (1992).
 ** Relative to the mean value over 28 points in typical grains with microprobe analyses at spinel phase. Standard deviations are given in parentheses.
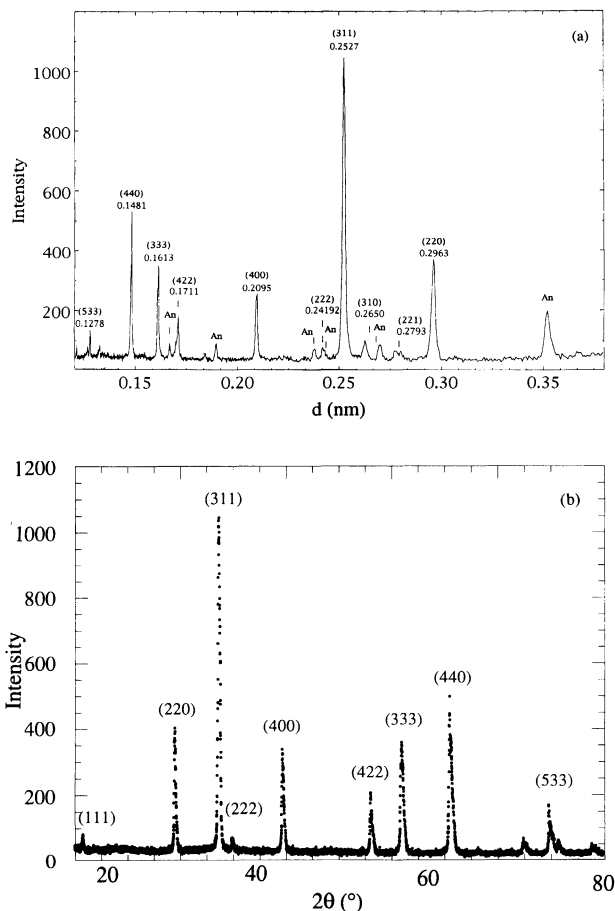

Fig. 1. (a) Powder X-ray patterns of the magnetically separated fraction plotted as a function of d. Fitted d positions and related (hkl) planes are indicated for the cubic spinel. An = anatase. (b) Pulverized Mg-rich maghemite crystals plotted as a function of scattering angle ($CuK\alpha$ radiation).

approximately 6 m of red soil, which is strongly magnetic (Carmo et al., 1984, Ferreira et al., 1994). The tuffite covers an area of the Bauru sandstone in the Mata da Corda formation. It is pyroclastic material derived from volcanic ash from a long-extinct source at Serra Negra.

The tuffite is porous and friable. It is easily reduced to a powder composed of micrometer-sized grains. Samples were taken from different levels, but no essential differences were observed. The overall chemical composition is given in Table 1. The composition is typical of a basalt that has been altered during an extended weathering process. Much of the Si, Al, and Na have been removed, while the K has been retained by clay minerals. Fe, Ti, and Cr contents are all high. X-ray diffraction indicated that the bulk of the tuffite is composed of poorly crystallized silicates, particularly nontronite. Gibbsite, anatase, and a spinel-type iron oxide were also detected. Traces of halloysite were identified by SEM.

The magnetic fraction was removed by high-gradient magnetic separation. Several (2–5) grams of tuffite were made into a dilute slurry in water and passed through a tube containing a mesh of steel wool (wire diameter 30 μm) placed in a uniform magnetic field of 0.3 T. The field was removed and the magnetic fraction washed out. The separate was typically 8% of the tuffite mass.

Examination of the magnetic extract by X-ray diffraction showed that the major phase was the spinel-type oxide. The lattice parameter a_0, equal to 0.8380(2) nm, was obtained by least-squares fit to the positions of five intense reflections measured using a Siemens D500 powder diffractometer with $CuK\alpha$ radiation (Fig. 1a). A Si standard was used for calibration. Primitive cubic cell reflections were not observed. A secondary phase was identified as anatase [a = 0.3790(3), c = 0.9503(3) nm]. Some submillimeter crystals with a recognizable octahe-

dral habit were identified in the optical microscope, and four were used for further magnetic analysis. The powder X-ray diffraction pattern for several small crystals is shown in Figure 1b.

Several samples were analyzed in a Leica Cambridge Stereoscan 360 scanning electron microscope equipped with an energy-dispersive X-ray spectrometer. Typical grain sections are illustrated in Figure 2, where the Ti-rich phase (anatase) is seen to be present as inclusions or intergrowths in some of the Fe-rich grains. Minor amounts of Si-rich secondary phases are also associated with some of the magnetic grains. The total amount of secondary phases in the magnetic extract is estimated at 30–40%.

Microprobe analysis

Chemical analyses at 28 points on 16 different crystals were obtained by energy-dispersive X-ray analysis. Results are included in Table 1. There is significant variation from grain to grain, but results within each grain are consistent. An average of all the 28 data points gives the

Fig. 2. Scanning electron micrograph showing a grain of Mg-rich maghemite (2) with anatase inclusion (1) and an associated silicate (3).

composition ($\square$ = vacancy) $Fe_{1.84}Mg_{0.41}Ti_{0.32}Al_{0.07}Cr_{0.03}Mn_{0.02}Si_{0.01}\square_{0.30}O_4$, with a molar mass of 0.1968 kg/mol. The Fe, Ti, and Mn are supposed to be in their highest oxidation states, Fe^{3+}, Ti^{4+}, and Mn^{4+}. The composition corresponds to a Mg-rich maghemite. All but two of the analyses show Mg > Ti. Analyses of the Ti-rich phase give a composition close to TiO_2.

Thermal analysis

No major exothermic reaction was observed by differential scanning calorimetry up to 500 °C. The X-ray diffraction pattern for the tuffite fired at 700 °C shows the continued presence of the spinel phase, which apparently does not convert to the corundum structure. The Curie temperature was measured by thermogravimetric analysis, using a thermobalance where the sample is subject to a nonuniform magnetic field of order 10 mT. Values of T_C are found to lie in the range 320–360 °C. A thermomagnetic curve up to 700 °C is shown in Figure 3a. It is essentially reversible, whereas the one for pure maghemite shown in Figure 3b for comparison exhibits an irreversible transformation to hematite at $T_x = 670$ °C. A fall in the room-temperature magnetization of the Mg-rich maghemite was observed after heating to 900 °C.

Magnetization

A typical room-temperature magnetization curve of a small octahedral crystal from the magnetic extract is shown in Figure 4. Data were obtained with a compact vibrating-sample magnetometer (Cugat et al., 1994). These curves were measured on four crystals with masses in the range 0.1–2.3 mg, and the saturation magnetization was deduced by extrapolating to $B_0 = 0$. Results are given in Table 2. Values range from 18 to 31 J/(T·kg) but the
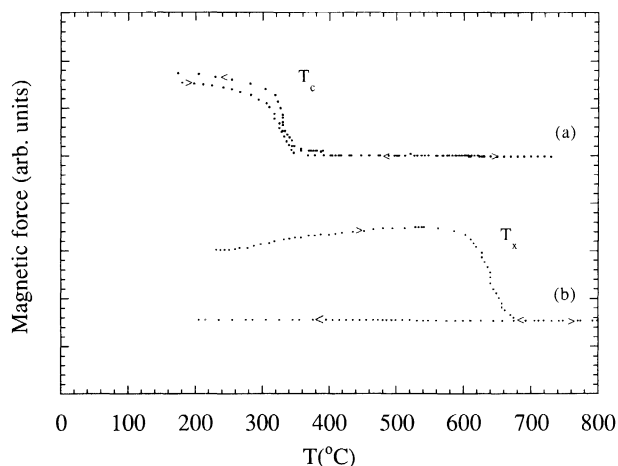

Fig. 3. Magnetic thermograms measured at 10 °C/min in air for (a) Mg-rich maghemite and (b) pure maghemite.

average is $\sigma_s = 25$ J/(T·kg). Using the X-ray estimated density, this corresponds to $M_s = 96$ kA/m. Similar values were obtained from the whole magnetic extract after correcting for the ~35 wt% of nonmagnetic secondary phases associated with the maghemite.

Mössbauer spectroscopy

The ^{57}Fe Mössbauer spectra at room temperature of the whole tuffite and the magnetic extract are shown in Figure 5. Spectra are also shown for the latter at 15 K and at room temperature in a field of 0.4 T applied parallel to the γ direction. The field is more than thrice that needed to saturate the magnetization (cf. Fig. 4; $\mu_0 M_s = 0.12$ T). The data were fitted by standard least-squares
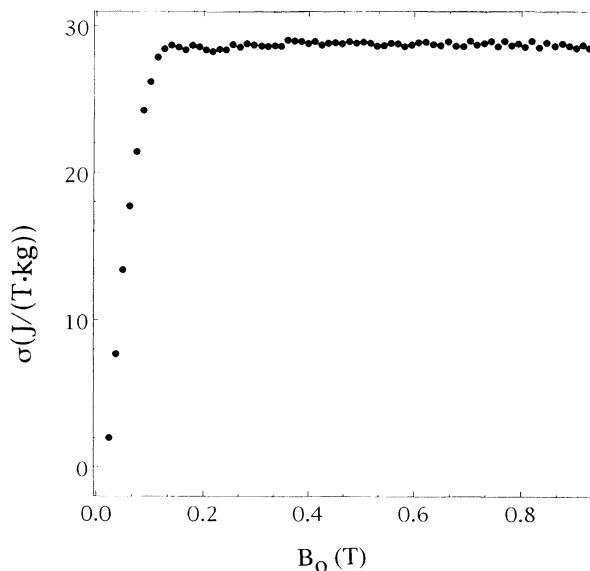

Fig. 4. The room-temperature magnetization curve of a single crystal of Mg-rich maghemite (mass 0.6 mg).

methods to two or three magnetic hyperfine patterns and a central quadrupole doublet. The spectra of magnetic extract at room temperature and 15 K show two strongly overlapping six-line patterns. Hyperfine fields at room temperature are 45.3 and 49.0 T, with relative intensity of 41.6:58.4, whereas at 15 K they are 50.8 and 53.0 T, with relative intensity of 47.6:52.4. They are attributed to Fe in A and B sites, respectively, of the spinel lattice. A small central peak is attributed to paramagnetic Fe present in silicates. The fit parameters are listed in Table 3. In the spectrum of the whole tuffite, the paramagnetic doublet is much more intense. There is no evidence of any Fe^{2+}. Less than 8% of the Fe in the magnetic extract is in the paramagnetic ferric form. Furthermore, the isomer shifts (IS) of the two hyperfine patterns associated with A and B sites are identical within 0.03 mm/s to those reported by da Costa et al. (1994) for γ-Fe_2O_3 at room temperature [IS Fe^{3+}(B) = 0.357 mm/s and IS Fe^{3+}(A) = 0.233 mm/s]. The difference IS(B) − IS(A) = 0.08 mm/s is also in good agreement with the reported value for maghemite (Pollard and Morrish, 1987; Vandenberghe and De Grave, 1989).

DISCUSSION

The magnetic phase is a cation-deficient ferric spinel containing Mg and Ti. The amount of vacancies is similar to that in the ideal maghemite formula, hence the oxide should be regarded as a form of maghemite rather than a variant of magnesioferrite $MgFe_2O_4$. In all but two of the 28 analyses summarized in Table 1 the second cation is Mg, so we refer to the phase as Mg-rich maghemite.

TABLE 2. Chemical composition and magnetic properties of four Mg-rich maghemite crystals

Chemical composition	T_c (°C)	σ_{exp} [J/(T·kg)]	σ_{col} [J/(T·kg)]
$Fe_{1.84}Ti_{0.34}Mg_{0.43}Al_{0.07}Si_{0.01}Mn_{0.02}\square_{0.29}O_4$	357	29	14
$Fe_{1.69}Ti_{0.35}Mg_{0.55}Al_{0.10}Si_{0.01}Mn_{0.01}\square_{0.29}O_4$	325	21	13
$Fe_{1.85}Ti_{0.34}Mg_{0.41}Al_{0.06}Si_{0.01}Mn_{0.02}\square_{0.31}O_4$	340	18	14
$Fe_{1.79}Ti_{0.41}Mg_{0.37}Al_{0.05}Si_{0.01}Mn_{0.01}\square_{0.36}O_4$	346	31	13

Note: each analysis is the average of four points.

Turning now to the cation distribution, there are vacancies and three major cations, Fe, Mg, and Ti, to distribute over the A and B sites. A definitive distribution of all four species cannot be achieved, but the main features of the distribution can be inferred with some confidence. Cation vacancies in pure maghemite are often considered to be located on B sites (Lindsley, 1976), therefore we place them there in the present mineral. The Fe(A):Fe(B) ratio [0.91(3)] is taken directly from the ratio of the A- and B-site Mössbauer intensities at 15 K. The Mg distribution in spinels depends on thermal history, but the distribution in quenched samples is close to random (Sawatzky et al., 1969a). Ti is known to have a strong B-site preference (Waychunas, 1991). Taking these factors into account, we suggest the average composition $[Fe_{0.88}Mg_{0.11}Si_{0.01}]\{Fe_{0.96}Mg_{0.30}Ti_{0.32}Al_{0.07}Cr_{0.03}Mn_{0.02}\square_{0.30}\}$-$O_4$, where [] denotes A sites, {} denotes B sites, and $\square$ denotes vacancies.

Assuming a collinear ferrimagnetic structure, with 5 μ_B per Fe^{3+} and 3 μ_B per Cr^{3+} or Mn^{4+} ion, the net magnetic

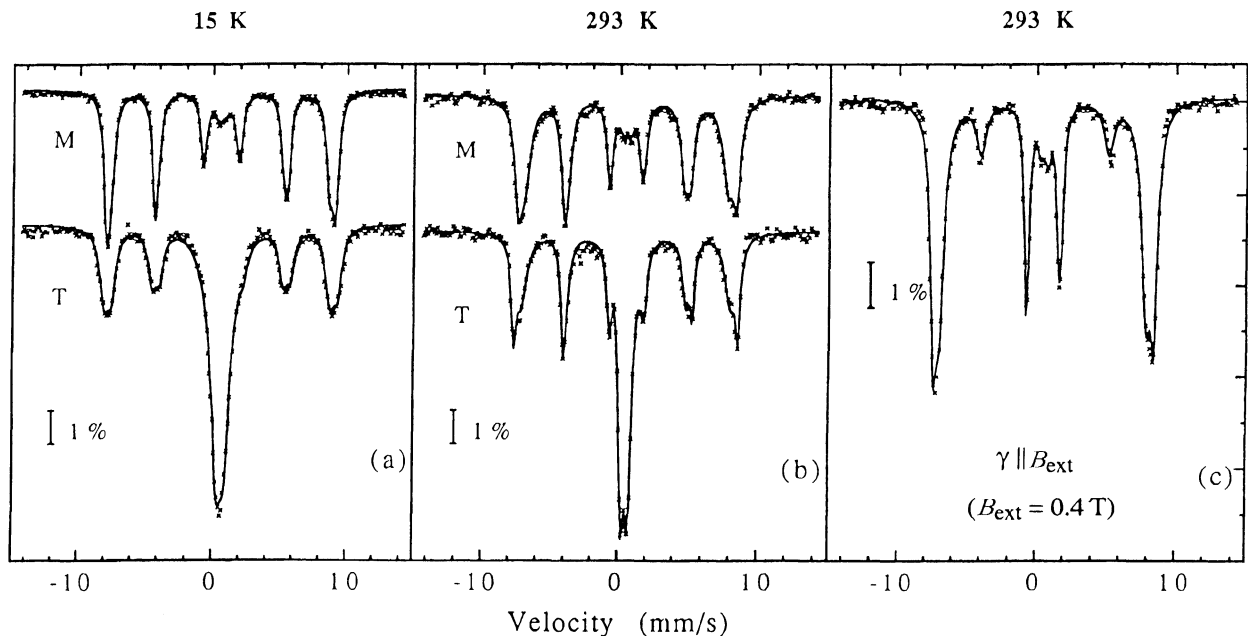15 K   293 K   293 K

Fig. 5. Mössbauer spectra for the magnetically separated (M) fraction and the whole tuffite sample (T) measured at (a) 15 K and (b) room temperature. (c) Mössbauer spectrum for the magnetically separated fraction measured in a 0.4 T externally applied magnetic field parallel to the γ direction at room temperature. The fits are shown with solid lines.

TABLE 3. Mössbauer parameters

Sample	T (K)	Parameters*	[Fe]	{Fe}	Para-mag-netic
HGMS extract	293	B_{hf} (T)	45.3	49.0	0
		IS (mm/s)	0.263	0.345	0.298
		QS (mm/s)	−0.002	−0.021	0.625
		LW (mm/s)	0.306	0.306	0.345
		RA (%)	38.9	54.6	6.6
	15	B_{hf} (T)	50.8	53.0	0
		IS (mm/s)	0.385	0.459	0.474
		QS (mm/s)	−0.019	−0.016	0.302
		LW (mm/s)	0.292	0.265	0.689
		RA (%)	44.0	48.4	7.6
Tuffite	293	B_{hf} (T)	46.2	50.2	0
		IS (mm/s)	0.260	0.359	0.349
		QS (mm/s)	−0.022	−0.150	0.494
		LW (mm/s)	0.250	0.250	0.290
		RA (%)	21.1	37.4	41.5
	15	B_{hf} (T)	52.1	52.2	0
		IS (mm/s)	0.144	0.708	0.463
		QS (mm/s)	0.025	−0.087	0.586
		LW (mm/s)	0.370	0.370	0.446
		RA (%)	25.7	28.4	45.8
HGMS extract**	293	B_{hf} (T)	46.2	49.2	0
		IS (mm/s)	0.275	0.389	0.380
		QS (mm/s)	0.020	−0.087	0.521
		LW (mm/s)	0.293	0.293	0.327
		RA (%)	36.1	58.2	5.7

Note: Mössbauer parameters for the high-gradient magnetically separated (HGMS) fraction (with and without 0.4 T externally applied magnetic field parallel to the γ direction) and the whole tuffite sample measured at room temperature and 15 K.

* B_{hf} = hyperfine field; QS = quadrupole splitting; IS = isomer shifts relative to α-Fe at room temperature; LW = line width; and RA = relative area of the subspectrum.

** B_{ext} = 0.4 T.

moment will be 0.55 μ_B per formula unit. The corresponding magnetization is 16 J/(T·kg). The measured values of magnetization σ_{exp} for the four crystals listed in Table 2 are systematically higher than the values σ_{col} calculated assuming a collinear ferrimagnetic structure and an Fe(A):Fe(B) ratio of 0.91. A possible difference in recoilless fractions (f) for the two sites has not been taken into account, as Fe nuclei in B sites have an f value 6% lower than in A sites at room temperature but are almost equal at 0 K, in pure Fe_3O_4 (Sawatzky et al., 1969b). The discrepancy between σ_{exp} and σ_{col} is partly attributable to the experimental error in determining the A:B ferric site occupancy from the Mössbauer spectrum. The calculated moment depends on the difference Fe(B) − Fe(A) of two quantities that are almost equal, and it is very sensitive to a small error in the Fe(A):Fe(B) ratio. The likely ranges of A- and B-site Fe contents per formula unit are 0.86–0.89 and 0.95–0.98, respectively. Taking into account these estimations, the expected value for σ_{col} is in the range of 13–21 J/(T·kg).

The Mössbauer spectrum at room temperature in the applied field of 0.4 T, which is clearly sufficient to saturate the magnetization (Fig. 4), indicates by the presence of residual intensity in lines 2 and 5 that the magnetic structure is not strictly collinear. These absorption lines are due to the $\Delta m = 0$ transition. Spin-canting-like structure is produced by the nonmagnetic cations on the op-

posite sublattice (Coey, 1987). In the present case, half the B sites are occupied by nonmagnetic cations or vacancies, favoring spin canting on A sites, which would also help to explain the larger than expected moments.

The thermal stability of Mg-rich maghemite may be related to the insolubility of Mg in α-Fe_2O_3. The stabilizing effect of Na, K, and Be on γ-Fe_2O_3 was first noted by Michel and Chaudron (1935).

Oxidation of titanomagnetite is often considered to be achieved by expulsion of Fe from the lattice. It is possible that oxidation of the present mineral has been achieved by expulsion of Ti, given the association with anatase, TiO_2.

In conclusion, a new cation-deficient ferric mineral of volcanic origin with the spinel structure having Mg > Ti has been described. The cation distribution with vacancies on B sites and a preference of Fe^{3+} for A sites is inferred from the Mössbauer and magnetization data. Like Ti and Al, the Mg substitution rapidly reduces the magnetization of maghemite. The mineral is the strongly magnetic constituent of certain magnetic soils. Unlike pure maghemite, its spinel structure is stable in air well above 700 °C.

REFERENCES CITED

Allan, J.E.M., Coey, J.M.D., and Sanders, I.S. (1989) An occurrence of a fully-oxidized natural titanomaghemite in basalt. Mineralogical Magazine, 53, 299–304.
Boudeulle, M., Batis-Landoulsi, H., Leclerq, C.-H., and Vergnon, P. (1983) Structure of γFe_2O_3 microcrystals: Vacancy distribution and structure. Journal of Solid State Chemistry, 48, 21–32.
Carmo, D.N., Curi, N., and Resende, M. (1984) Caracterização e gênese de latossolos da região do Alto Paranaíba (MG). Revista Brasileira de Ciência do Solo, 8, 235–240.
Coey, J.M.D. (1987) Noncollinear spin structures. Canadian Journal of Physics, 65, 1210–1232.
Cugat, O., Byrne, R., Macaulay, J., and Coey, J.M.D. (1994) A compact vibrating-sample magnetometer with variable permanent magnetic flux source. Review of Scientific Instruments, 65, 3570–3573.
da Costa, G.M., De Grave, E., Bowen, L.H., Vandenberghe, R.E., and de Bakker, P.M.A. (1994) The center shift in Mössbauer spectra of maghemite and aluminium maghemites. Clays and Clay Minerals, 42, 628–633.
Ferreira, S.A.D., Santana, D.P., Fabris, J.D., Curi, N., Nunes Filho, E., and Coey, J.M.D. (1994) Relação entre magnetização, elementos traços e litologia de duas seqüências de solos de estado de Minas Gerais. Revista Brasileira de Ciência do Solo, 18, 167–174.
Fontes, M.F. (1992) Chemical and mineralogical analyses of a weathering sequence of tuffite from the region of Patos de Minas (MG), Brazil, 92 p. M.Sc. thesis, Universidade Federal de Viçosa, Minas Gerais, Brazil (in Portuguese).
Gillot, B., and Benloucif, R.M. (1992) X-ray diffraction, IR spectrometry and high resolution electron microscopy on ordered zinc-substituted maghemites. Materials Chemistry and Physics, 32, 37–41.
Goss, C.J. (1988) Saturation magnetization, coercivity and lattice parameter changes in the system Fe_3O_4-γFe_2O_3 and their relationship to structure. Physics and Chemistry of Minerals, 16, 164–171.

Greaves, C. (1983) A powder neutron diffraction investigation of vacancy and covalence in γ-ferric oxide. Journal of Solid State Chemistry, 30, 257–263.

Lindsley, D.H. (1976) The crystal chemistry and structure of oxide minerals as exemplified by the Fe-Ti oxides. In Mineralogical Society of America Reviews in Mineralogy, 3, L1–L60.

Michel, A., and Chaudron, G. (1935) Étude du sesquioxide de fer cubique stabilisé. CR Académie des Sciences, 186, 1191–1193.

Moukarika, A., O'Brien, F., Coey, J.M.D., and Resende, M. (1991) Development of magnetic soil from ferroan dolomite. Geophysical Research Letters, 18, 2043–2046.

Pollard, R.J., and Morrish, A.H. (1987) High-field magnetism in nonpolar maghemite recording particles. IEEE Transactions on Magnetics, vol. MAG-23(1), 42–44.

Prévot, M., Lecaille, A., and Mankinen, E.A. (1981) Magnetic effects of maghemitization of ocean crust. Journal of Geophysical Research, 86, 4009–4020.

Readman, P.W., and O'Reilly, W. (1972) Magnetic properties of oxidized (cation-deficient) titanomaghemites $(Fe,Ti)_3O_4$. Journal of Geomagnetism and Geoelectricity, 24, 69–90.

Resende, M., Allan, J., and Coey, J.M.D. (1986) The magnetic soils of Brazil. Earth and Planetary Science Letters, 78, 322–326.

Sawatzky, G.A., Van Der Woude, F., and Morrish, A.H. (1969a) Mössbauer study of several ferrimagnetic spinels. Physical Review, 187, 747–757.

——— (1969b) Recoilless-fraction ratios for Fe^{57} in octahedral and tetrahedral sites of a spinel and a garnet. Physical Review, 183, 383–386.

Schwertmann, U., and Fechter, H. (1984) The influence of aluminum on iron oxides: XI. Aluminum-substituted maghemite in soils and its formation. Soil Society of America Journal, 48, 1462–1463.

Smith, P.P.K. (1979) The observation of enantiomorphous domains in natural maghemite. Contributions to Mineralogy and Petrology, 69, 249–254.

Vandenberghe, R.E., and De Grave, E. (1989) Mössbauer effect studies of oxidic spinels. In G.L. Long and F. Grandjean, Eds., Mössbauer spectroscopy applied to inorganic chemistry, vol. 3, p. 59–172. Plenum, New York.

Waychunas, G.A. (1991) Crystal chemistry of oxides and oxyhydroxides. In Mineralogical Society of America Reviews in Mineralogy, 25, 11–68.